Clinical Ophthalmology

Dovepress
Taylor & Francis Group

Open Access Full Text Article

SHORT REPORT

Tear Biomarkers of Topical Sirolimus in Meibomian Gland Dysfunction: A Randomized Trial

Lei Zhou[1,2,*], Hiroyuki Shimizu[3,*], Yuki Togashi[3], Tomoko Kirihara[3], Yuhan Yang[4], Chuen Thomas Lam[2,5], Hisao Shimada[3], Louis Tong[6,7]

[1]School of Optometry, Department of Applied Biology and Chemical Technology, Research Centre for SHARP Vision (RCSV), The Hong Kong Polytechnic University, Hong Kong, People's Republic of China; [2]Centre for Eye and Vision Research (CEVR), Hong Kong, People's Republic of China; [3]Santen Pharmaceutical Co., Ltd., Osaka, Japan; [4]School of Optometry, The Hong Kong Polytechnic University, Hong Kong, People's Republic of China; [5]Centre for Myopia Research, School of Optometry, Research Centre for SHARP Vision (RCSV), Research Centre for Chinese Medicine Innovation (RCMI), The Hong Kong Polytechnic University, Hong Kong, People's Republic of China; [6]Singapore Eye Research Institute, Singapore, Singapore; [7]Singapore National Eye Centre, Singapore, Singapore

*These authors contributed equally to this work

Correspondence: Louis Tong, Singapore National Eye Centre, 11 Third Hospital Avenue, Singapore, 168751, Singapore, Tel +6598186221, Email Louis.tong.h.t@singhealth.com.sg

Purpose: Pharmacodynamic biomarkers of sirolimus were investigated using omics analysis of tear fluids from Japanese patients with meibomian gland dysfunction (MGD).

Methods: In a Phase 2a trial, sirolimus or vehicle eyedrops were administered twice daily for 12 weeks. Tear samples from 29 patients (15 sirolimus, 14 vehicle) were collected pre- and post-treatment. LC-MS/MS-based proteomics and lipidomics were performed. Within-group changes were analyzed, followed by differential expression and pathway analysis. Key candidates were evaluated using estimation plots (Registration ID: UMIN000049186).

Results: Over 3000 proteins and 55 lipids were quantified. mTOR signaling components (ATP6V1D, RRAGC, DEPTOR) were significantly modulated. ATP6V1D showed a significant decrease in the sirolimus group ($p = 0.0024$), but not in the vehicle group ($p = 0.528$). Lipids 12-HETE and 13-HpODE significantly increased post-treatment in the sirolimus group.

Conclusion: Results suggested that sirolimus inhibited the mTOR pathway. ATP6V1D, 12-HETE, and 13-HpODE were suggested to be pharmacodynamic biomarkers for sirolimus. These findings may facilitate pharmacodynamic monitoring of mTOR-targeted therapies for ocular surface disorders.

Keywords: MGD, pharmacodynamic biomarker, tear fluid sample, mTOR inhibitor

Introduction

Meibomian gland dysfunction (MGD) is a condition marked by diffuse abnormalities in meibomian gland function and chronic ocular discomfort. It is classified into low- and high-delivery types, with clinical features including symptoms, eyelid margin irregularities, and meibum secretion issues.[1,2] MGD is a major cause of evaporative dry eye, and most patients with dry eye have underlying MGD.[3] Prevalence varies by region—32.9% in Japan,[4] 56.3% in Singapore,[5] and 21.2% in the U.S.[6] — with differences in diagnostic criteria and environmental exposure likely contributing to the higher apparent prevalence in Asia. Inflammation and environmental stressors like oxidative damage and apoptosis are known contributors.[2]

Current treatments include eyelid hygiene, warm compresses, thermal pulsation, light therapies, probing, and medications like doxycycline and azithromycin.[7] While effective, these methods face limitations such as poor adherence

https://doi.org/10.2147/OPTH.S514118
Received: 18 September 2025
Accepted: 9 February 2026
Published: 27 March 2026

and high costs. Eye drops offer a more accessible alternative, but existing options like azithromycin may cause irritation and antibiotic resistance concerns,[8] and no eye drops are yet approved specifically for MGD.[7]

Sirolimus, an mTOR inhibitor, was evaluated in a Phase 2a trial for MGD. Given the limitations of clinical endpoints —such as symptom scores and tear breakup time (TBUT), which may not fully capture the efficacy of interventions in MGD—, pharmacodynamic (PD) biomarkers are valuable for clarifying its biological effects. Sirolimus has broader therapeutic potential, including cancer research, making PD marker development especially important.

Omics-based analyses enable system-level understanding of tear composition changes in response to treatment. Tear fluid is a promising source for biomarker discovery due to its proximity to the disease site and ease of collection. It contains 6–11 mg/mL of protein and over 2000 distinct proteins.[9] Besides, hundreds of lipids have also been recorded across seven lipid classes.[10] Proteomics has already advanced understanding of dry eye disease,[11] and lipid biomarkers have been studied in MGD.[12]

This study aimed to identify PD markers for sirolimus by analyzing proteins and lipids from Phase 2a trial participants.

Materials and Methods

Study Design

This exploratory study aimed to identify candidate PD markers using tear fluid samples from clinical trial participants who provided informed consent. Study details and opt-out instructions were made available on the local website of Santen Pharmaceutical Co., Ltd. (Osaka, Japan), ensuring easy patient access. The study complied with the Declaration of Helsinki and was approved by the ethics committee of Santen Pharmaceutical Co., Ltd. (No. RINRI-2022-008). It was registered with the University Hospital Medical Information Network Clinical Trials Registry (UMIN000049186).

Subjects

Tear fluid samples were obtained from patients in a randomized, multicenter, evaluator-masked, vehicle-controlled Phase 2a study in Japan. Detailed information was described separately in Supplementary Material 1. Patientswere randomly assigned to receive sirolimus or vehicle eyedrops twice daily in both eyes, along with daily warm compresses, over a 12-week period. Tear profiles from 29 subjects (15 sirolimus, 14 vehicle) were analyzed. This tear fluid study was exploratory, and the number of samples was determined by the number of subjects enrolled in the Phase 2a study.

Tear Collection

Tear fluid samples derived from both eyes were collected twice—before treatment and 10 weeks after randomization—using Schirmer's test strips without local anesthesia. The strips were placed under the eyelid, the wetted length measured, and then immediately frozen at −80 °C until analysis for this study. The storage duration before analysis was up to 1.5 years, and no freeze–thaw cycles occurred prior to measurement.

Extraction of Proteins and Lipids

Schirmer's strips were longitudinally halved, with one half used for proteomics and the other for lipidomics analysis.

Sample Preparation for Proteomics

Strips were cut into small pieces and lysed in 100 µL buffer using a Thermomixer (1.5 h, 20 °C) and the samples were centrifuged at 14,000 g. Protein concentration was measured using the Bio-Rad DC Protein assay. A total of 100 µg of tear proteins were reduced, alkylated, digested with trypsin, and desalted using Thermo Easy Mini sample prep kits (ThermoFisher Scientific, San Jose, CA). Peptides were quantified using a fluorometric peptide quantification kit (ThermoFisher Scientific).

Sample Preparation for Lipidomics

Strips were extracted in 980 µL methanol containing 10 µL of 0.2 mg/mL BHT (antioxidant) and 10 µL of internal standard solution (composition in Supplementary Material 2). After overnight incubation at 4 °C, samples were

centrifuged (14,000 g, 10 min, 4 °C), and supernatants were dried and reconstituted in 80 µL of water:acetonitrile (6:4, v/v) with 0.1% acetic acid. A triple quadrupole LC-MS/MS system (Agilent UHPLC 1290 linked to an Agilent 6495C QQQ) was used for analysis, and the instrument was tuned prior to each batch analysis. Analytes were chromatographically separated on a Phenomenex Kinetex C8 column (2.1×150 mm, 2.6 um) with the following mobile phases: water + 0.1% formic acid (A) and acetonitrile + 0.1% formic acid (B) at 40°C. A pooled lipid extract served as a QC sample and was injected every five study samples.

Quantitative Proteomics Analysis

Peptides were dried (SpeedVac), resuspended in 0.1% FA/2% ACN with iRT (1:10, Biognosys), and analyzed using an EASY-nLC 1200 system coupled to an Orbitrap Exploris™ 480 Mass Spectrometer (ThermoFisher Scientific). LC separation was performed using Acclaim PepMap 100 C18 (pre-column) and PepMap® RSLC C18 (analytical column) with a 60-minute gradient of buffer A (0.1% FA) and buffer B (80% ACN in 0.1% FA). DIA-based proteomics used 19 windows of 45.7 Da with 3 Da overlap. AGC target was 1000%, and injection time was set to auto. Data were processed using Spectronaut 15's library-free directDIA workflow. Normalization was based on total protein concentration.

Quantitative Lipidomics Analysis

The LC-MS/MS analysis was conducted using an Agilent UHPLC 1290 Infinity II system coupled with an Agilent QqQ 6495C. Reverse-phase separation was performed on a Phenomenex Kinetex C8 column (2.1 × 150 mm, 2.6 µm) with mobile phases A (water + 0.1% formic acid) and B (acetonitrile + 0.1% formic acid). The gradient program was summarized in Supplementary Material 3. Column temperature was 40°C, flow rate 0.4 mL/min, and injection volume 20 µL.

Positive ionization was applied with spray and nozzle voltages of 3000 V and 1000 V, respectively. Drying and sheath gas temperatures were 250°C, with flow rates of 14 L/min and 11 L/min. Nebulizer pressure was 35 psi. iFunnel RF voltages were 150 V (high) and 60 V (low). Targeted analysis was performed in dynamic MRM positive ion mode.

MS data were analyzed using Agilent MassHunter (version B.10.00). Signal-to-noise ratios (S/N) were calculated from raw peak areas in study samples and processed blanks. Lipids with S/N < 10, CV > 20% in QC samples, or poor linearity ($R^2 < 0.8$) in dilution curves were excluded. Raw peak areas were normalized using internal standards, and concentrations were adjusted based on the wet length of strips.

Statistical Analysis

The proteomic data analysis and data visualization were carried out using custom R (64-bit version 4.1.1). The DIA intensities were median-normalized and log-transformed. Visualization included volcano plots, heatmaps, and OPLS-DA to compare tear proteomic profiles before and after treatment in both sirolimus and vehicle groups. Gene ontology (GO) and protein-protein interaction (PPI) network analysis were performed using Metascape.[13] Estimation plots were generated via https://www.estimationstats.com/#/. Similar approach was used for lipidomics data analysis.

Results

The demographics of the participant are shown in Table 1. A total of 116 tear fluid samples (Pre-treatment: 58 samples, Post-treatment: 58 samples) derived from 29 subjects were included in this study.

Table 1 Patient Demographics

		Vehicle	Sirolimus	P-value
Number		14	15	–
Female	%	50	73	–
	Portion	7/14	11/15	P= 0.26
Age	Mean ± SD	54 ± 11	55 ± 12	P=0.82

Notes: Female proportion was compared using Fisher's exact test; age was compared using Welch's *t*-test.

Proteomics

A total of 3305 unique tear proteins were identified (false discovery rate, FDR < 0.01) and quantified. Differential expression profiles between vehicle and sirolimus groups were visualized using volcano plots, with fold change defined as the post-/pre-treatment expression ratio. Proteins exhibiting fold changes >1.5 or <0.67 with p < 0.05 (paired *t*-test, unadjusted) were considered significantly modulated, identifying 51 upregulated and 76 downregulated proteins (Figure 1A). Unsupervised clustering of the top 25 differentially expressed proteins in the sirolimus group revealed distinct post-treatment proteomic signatures (Figure 1B), further supported by an R2Y value of 0.966 from orthogonal partial least squares discriminant analysis (OPLS-DA) (Figure 1C).

Gene Ontology enrichment analysis of 127 dysregulated proteins identified multiple significant biological processes (Figure 2A). Given sirolimus's role as an mTOR pathway inhibitor, the M121 "PID_MTOR_4PATHWAY" was focused on. Protein-protein interaction (PPI) network analysis highlighted ATP6V1D, RRAGC, and DEPTOR as key nodes (Figure 2B and C). Among these, ATP6V1D exhibited a statistically significant reduction in post-treatment samples from the sirolimus group (mean difference: −1.04e+04, 95% CI: −1.55e+04 to −4.78e+03; p = 0.0024, two-sided permutation *t*-test), whereas no significant change was observed in the vehicle group (mean difference: 2.74e+03, 95% CI: −6.8e+03 to 9.85e+03; p = 0.528) (Figure 2D).

Lipidomics

A total of 55 unique lipids were quantified. Volcano plots visualized significant differential profiles between pre- and post-treatment in vehicle and sirolimus groups. Using fold change >1.2 or <0.83 and p<0.05 (paired non-parametric *t*-test), two

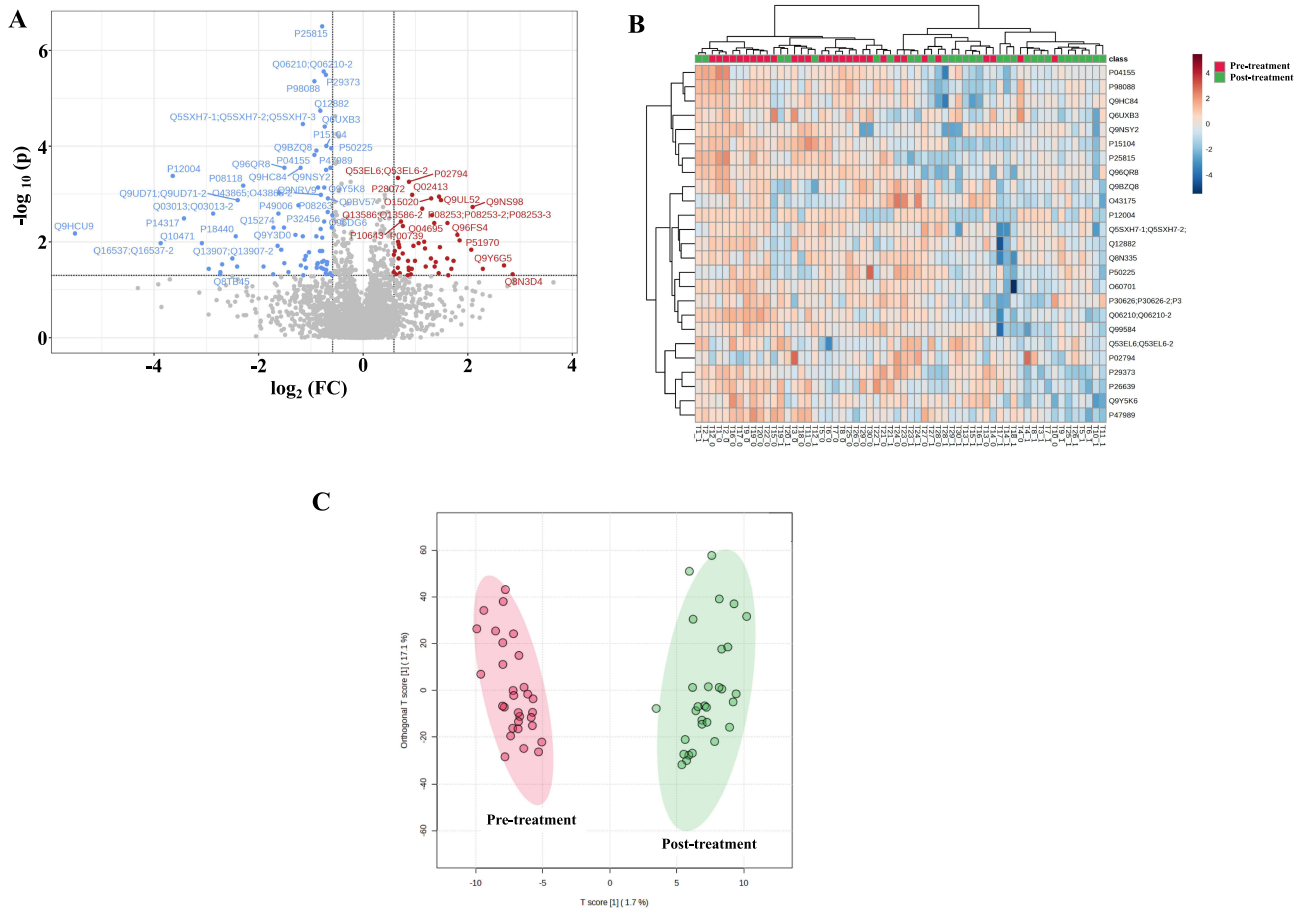

Figure 1 (**A**) Volcano plot shows the significantly dysregulated proteins in tears by comparing post-treatment to pre-treatment in sirolimus group. The cutoffs for significant changes are FC of 1.5 and p-value < 0.05 (paired *t*-test, unadjusted); (**B**) Heatmap visualization of tear protein profiles of post-treatment vs pre-treatment in sirolimus group. Top 25 significantly dysregulated tear proteins are shown based on paired *t*-test; (**C**) OPLS-DA score plot shows the separation of post-treatment and pre-treatment in sirolimus group (R2X (cum) = 0.314, R2Y(cum) = 0.966). Permutation test shows the OPLS-DA model is valid (p-value < 0.01).

https://doi.org/10.2147/OPTH.S514118

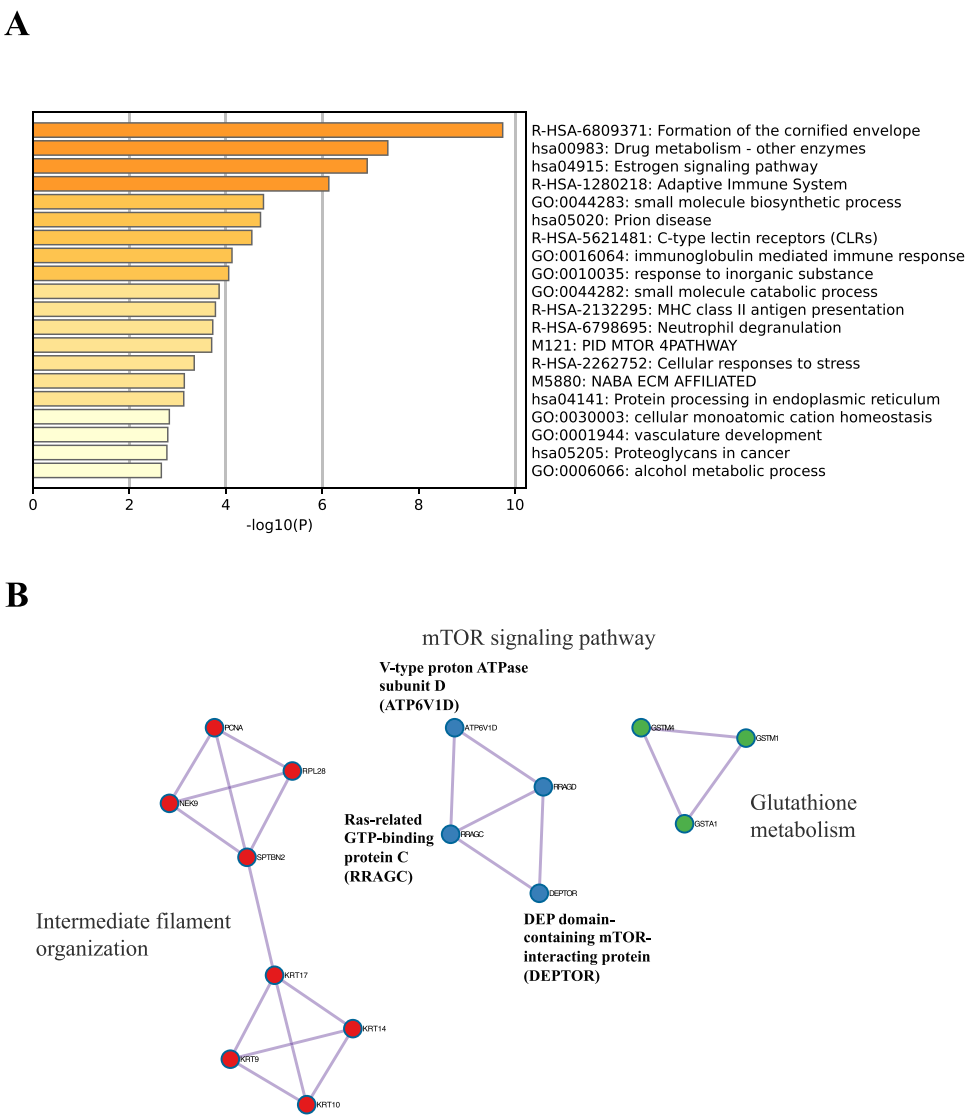

Figure 2 continued.

https://doi.org/10.2147/OPTH.S514118

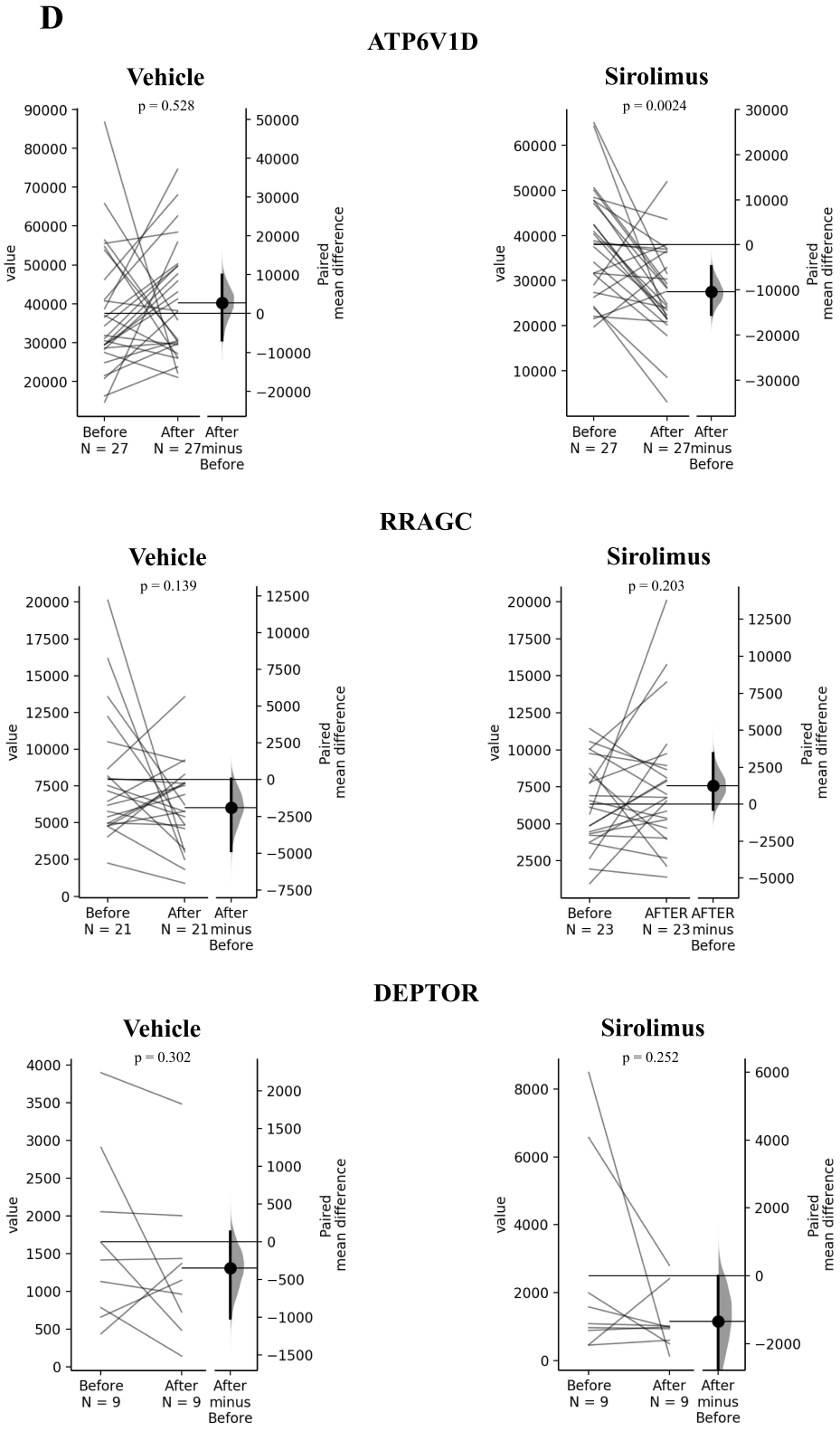

Figure 2 (**A**) Enriched gene ontology (GO) analysis was performed based on 127 dysregulated tear proteins using GO terms, KEGG, and Reactome database. mTOR signaling pathway (M121, PID_MTOR_4PATHWAY) was found to be one of the enriched pathways. PID refers to the Pathway Interaction Database, which provides curated signaling pathways, and M121 is the identifier for PID_MTOR_4PATHWAY in MSigDB; (**B**) Protein-protein interaction (PPI) network analysis also indicated that mTOR signaling pathway (ATP6V1D, RRAGC, and DEPTOR) is one of the three enriched modules; (**C**) PPI network shows mTORC1 signaling pathway (ATP6V1D, RRAGC, and DEPTOR) using STRING; (**D**) Estimation plots of ATP6V1D, RRAGC, and DEPTOR for post-treatment and pre-treatment in both sirolimus and vehicle groups. Two-sided permutation paired *t*-test was used.

https://doi.org/10.2147/OPTH.S514118

lipids (13-HpODE, 12-HETE) were up-regulated and two (5-HEPE, 15-HEPE) down-regulated post-treatment (Figure 3A). All statistical comparisons in the lipidomics analysis were performed using non-parametric tests. OPLS-DA score plot (Figure 3B) showed less separation between pre- and post-treatment groups than in proteomics (Figure 1C). Two-sided

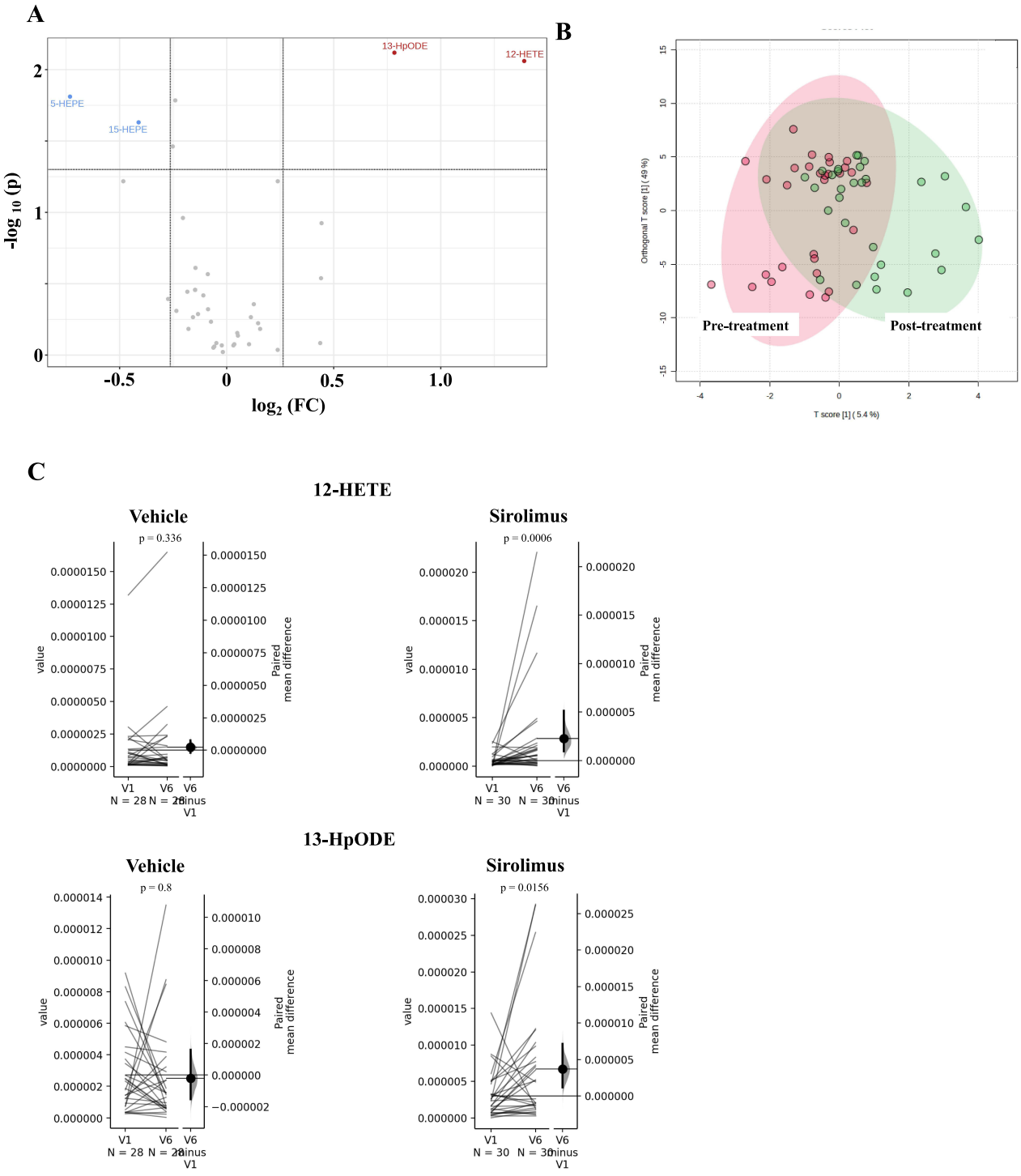

Figure 3 (**A**) Volcano plot revealed two upregulated lipids (13-HpODE and 12-HETE) and two downregulated lipids (5-HEPE and 15-HEPE) in tears by comparing post-treatment to pre-treatment in sirolimus group. The cutoffs for significant changes are FC of 1.2 and p-value < 0.05 (paired *t*-test, non-parametric); (**B**) OPLS-DA score plot shows the separation of post-treatment and pre-treatment in sirolimus group (R2X(cum) = 0.545, R2Y(cum) = 0.366). Permutation test shows the OPLS-DA model is still valid (p-value < 0.01) though some overlap was observed between the post-treatment group and the pre-treatment group; (**C**) Estimation plots of 12-HETE and 13-HpODE for post-treatment and pre-treatment in both sirolimus and vehicle groups. Two-sided permutation paired *t*-test was used.

https://doi.org/10.2147/OPTH.S514118

permutation paired t-tests confirmed 13-HpODE and 12-HETE were significantly elevated post-treatment in the sirolimus group (p=0.0156, p=0.0006), but not in the vehicle group (p=0.8, p=0.336) (Figure 3C). 5-HEPE and 15-HEPE showed no significant changes in either group (estimation plots not shown here).

Discussion

This study is among the first to apply integrated tear proteomics and lipidomics to assess the pharmacodynamic impact of topical sirolimus in MGD. Proteomic analysis quantified over 3000 tear proteins, identifying three mTOR-related proteins as sirolimus-responsive biomarkers. Among them, ATP6V1D was significantly reduced in the sirolimus group versus vehicle. Lipidomic profiling revealed significant elevation of 12-HETE and 13-HpODE following sirolimus treatment.

The ATP6V1 family is known to be involved in the regulation of intracellular pH, lipid metabolism, and inflammatory signaling during tumor progression,[14] and these processes are also related to the pathophysiology of MGD.[2,3] In particular, ATP6V1C1 has been reported to promote breast cancer growth via mTORC1 activation through increased V-ATPase activity.[15] In this study, the observed decrease in ATP6V1D expression following sirolimus administration (Figure 2D) is considered to suggest inhibition of the mTOR pathway, and it is suggested that this may regulate proton transport and restore lipid homeostasis and inflammatory balance in the meibomian gland, potentially contributing to improved gland function and reduced inflammation in MGD.

12-HETE, a metabolite of 12-lipoxygenase (12-LOX), is involved in tumorigenesis and cancer proliferation.[16,17] It also inhibits apoptosis via ILK/NF-κB activation in ovarian cancer cells.[18] Since activation of the NF-κB pathway is also involved in antioxidant responses, it is suggested that sirolimus-mediated mTOR inhibition may influence local lipid mediator dynamics and contribute to the suppression of inflammation and apoptosis in MGD. Conversely, 13-HpODE, known to induce endothelial cell apoptosis,[19] was significantly elevated in the sirolimus-treatment group (Figure 3C). Although 13-HpODE, a linoleic acid–derived hydroperoxide, has been linked to apoptosis, this increase may not directly indicate such an effect. Given that linoleic acid is elevated in meibomian gland secretions in MGD,[20] and that mTOR inhibition could plausibly alter lipid metabolism and promote 13-HpODE formation via the lipoxygenase pathway, the observed increase likely reflects these combined influences rather than serving as a simple marker of apoptosis. Taken together, the simultaneous elevation of both anti-apoptotic (12-HETE) and pro-apoptotic (13-HpODE) lipid mediators may reflect a complex regulatory response to mTOR inhibition in the ocular surface, highlighting the need for further investigation into their roles in MGD pathophysiology.

The current available treatment for MGD is warm compress or thermopulsation (LipiFlow). Ambaw et al reported significant reductions in 18 tear lipids following treatment.[21] However, as warm compresses were used continuously in both study arms, the specific contribution of eyelid warming could not be distinguished.

This study has two main limitations. First, the design: warm compress in both groups may confound the relationship between PD marker changes and clinical findings such as gland plugging, and the small sample size limits statistical power and generalizability. Second, analytical factors: inter-individual variability in tear fluid composition may affect biomarker consistency and interpretation. Future studies should control treatment conditions and include larger cohorts to improve robustness.

In conclusion, sirolimus treatment in MGD patients led to mTOR pathway inhibition, as shown by reduced ATP6V1D expression. Lipidomics identified 12-HETE and 13-HpODE as pharmacodynamic markers, reflecting changes in apoptosis, lipid metabolism, and inflammation in MGD. Importantly, identifying tear-based PD markers provides a foundation for objective assessment of mTOR-targeted therapy in ocular diseases.

Acknowledgments

The authors would like to thank Reiko Arita, MD, PhD. (Department of Ophthalmology, Itoh Clinic, Saitama, Japan) for evaluating the number of plugging of gland orifice to check the correlation with identified PD markers. This manuscript received partial assistance from Microsoft Copilot. All content was approved by the authors. The abstract of this paper was presented at the ARVO 2024 Annual Meeting as a poster presentation. The abstract was published in 'Poster

Abstracts' in Investigative Ophthalmology & Visual Science: https://iovs.arvojournals.org/article.aspx?articleid=2800337.

Funding

Supported by grants from Santen, Industry Alignment Fund – Industry Collaboration Project (I1701E0008), InnoHK initiative of the Innovation and Technology Commission of the Hong Kong Special Administrative Region Government, and PolyU grant P0043882.

Disclosure

Louis Tong received a financial support from Alcon, Novartis, Bausch and Lomb, Abbvie, Vivavision Biotech and Santen. Lei Zhou, Yuhan Yang, and Thomas Chuen Lam received a financial support from Santen. Hiroyuki Shimizu, Yuki Togashi, Tomoko Kirihara, and Hisao Shimada are employees of Santen. The authors report no other conflicts of interest in this work.

References

1. Tomlinson A, Bron AJ, Korb DR, et al. The international workshop on meibomian gland dysfunction: report of the diagnosis subcommittee. *Invest Ophthalmol Vis Sci*. 2011;52(4):2006–2049. doi:10.1167/iovs.10-6997f
2. Amano S, Shimazaki J, Yokoi N, et al. Meibomian gland dysfunction clinical practice guidelines. *Jpn J Ophthalmol*. 2023;67(4):448–539. doi:10.1007/s10384-023-00995-8
3. Stapleton F, Argüeso P, Asbell P, et al. TFOS DEWS III. *Digest Am J Ophthalmol*. 2025;279:451–553.
4. Arita R, Mizoguchi T, Kawashima M, et al. Meibomian gland dysfunction and dry eye are similar but different based on a population-based study: The Hirado-Takushima Study in Japan. *Am J Ophthalmol*. 2019;207:410–418. doi:10.1016/j.ajo.2019.02.024
5. Siak JJ, Tong L, Wong WL, et al. Prevalence and risk factors of meibomian gland dysfunction: the Singapore Malay eye study. *Cornea*. 2012;31(11):1223–1228. doi:10.1097/ICO.0b013e31823f0977
6. McCann P, Abraham AG, Mukhopadhyay A, et al. Prevalence and incidence of dry eye and meibomian gland dysfunction in the United States: a systematic review and meta-analysis. *JAMA Ophthalmol*. 2022;140(12):1181–1192. doi:10.1001/jamaophthalmol.2022.4394
7. Sheppard JD, Nichols KK. Dry eye disease associated with meibomian gland dysfunction: focus on tear film characteristics and the therapeutic landscape. *Ophthalmol Ther*. 2023;12(3):1397–1418. doi:10.1007/s40123-023-00669-1
8. Tao T, Tao L. Systematic review and meta-analysis of treating meibomian gland dysfunction with azithromycin. *Eye*. 2020;34(10):1797–1808. doi:10.1038/s41433-020-0876-2
9. Zhou L, Beuerman RW. The power of tears: how tear proteomics research could revolutionize the clinic. *Expert Rev Proteomics*. 2017;14(3):189–191. doi:10.1080/14789450.2017.1285703
10. Butovich IA. Tear film lipids. *Exp Eye Res*. 2013;117:4–27. doi:10.1016/j.exer.2013.05.010
11. Kannan R, Das S, Shetty R, Zhou L, Ghosh A, Deshpande V. Tear proteomics in dry eye disease. *Indian J Ophthalmol*. 2023;71(4):1203–1214. doi:10.4103/IJO.IJO_2851_22
12. Asiedu K. Candidate molecular compounds as potential indicators for meibomian gland dysfunction. *Front Med*. 2022;9:873538. doi:10.3389/fmed.2022.873538
13. Zhou Y, Zhou B, Pache L, et al. Metascape provides a biologist-oriented resource for the analysis of systems-level datasets. *Nat Commun*. 2019;10(1):1523. doi:10.1038/s41467-019-09234-6
14. Stransky L, Cotter K, Forgac M. The function of V-ATPases in cancer. *Physiol Rev*. 2016;96(3):1071–1091. doi:10.1152/physrev.00035.2015
15. McConnell M, Feng S, Chen W, et al. Osteoclast proton pump regulator Atp6v1c1 enhances breast cancer growth by activating the mTORC1 pathway and bone metastasis by increasing V-ATPase activity. *Oncotarget*. 2017;8(29):47675–47690. doi:10.18632/oncotarget.17544
16. Jiang Y, Pan Y, Rhea PR, et al. A sucrose-enriched diet promotes tumorigenesis in mammary gland in part through the 12-lipoxygenase pathway. *Cancer Res*. 2016;76(1):24–29. doi:10.1158/0008-5472.CAN-14-3432
17. Chang J, Jiang L, Wang Y, et al. 12/15 Lipoxygenase regulation of colorectal tumorigenesis is determined by the relative tumor levels of its metabolite 12-HETE and 13-HODE in animal models. *Oncotarget*. 2015;6(5):2879–2888. doi:10.18632/oncotarget.2994
18. Liu Q, Tan W, Che J, et al. 12-HETE facilitates cell survival by activating the integrin-linked kinase/NF-κB pathway in ovarian cancer. *Cancer Manag Res*. 2018;10:5825–5838. doi:10.2147/CMAR.S180334
19. Ryman VE, Packiriswamy N, Sordillo LM. Apoptosis of endothelial cells by 13-HPODE contributes to impairment of endothelial barrier integrity. *Mediators Inflamm*. 2016;2016:9867138. doi:10.1155/2016/9867138
20. Arita R, Mori N, Shirakawa R, et al. Linoleic acid content of human meibum is associated with telangiectasia and plugging of gland orifices in meibomian gland dysfunction. *Exp Eye Res*. 2016;145:359–362. doi:10.1016/j.exer.2016.02.005
21. Ambaw YA, Fuchs D, Raida M, et al. Changes of tear lipid mediators after eyelid warming or thermopulsation treatment for meibomian gland dysfunction. *Prostaglandins Other Lipid Mediat*. 2020;151:106474. doi:10.1016/j.prostaglandins.2020.106474